Positive-parity rotational bands in odd-A pf-shell nuclei: A shell model description

Alfredo Poves and Jorge Sánchez Solano
Departamento de Física Teórica, Universidad Autónoma, Cantoblanco, 28049 Madrid, Spain
(Received 10 February 1998)

Low-lying positive-parity rotational bands have been recently found in odd-A nuclei of the pf shell. Their occurrence can be explained as due to the coupling of a hole in the $1d_{3/2}$ orbit to the more deformed even-even pf-shell configurations. Shell model calculations in the full pf shell plus one hole in the $1d_{3/2}$ orbit for ^{47}V$-(1d_{3/2}\otimes{}^{48}$Cr)—and for ^{45}Sc$-(1d_{3/2}\otimes{}^{46}$Ti)—support this interpretation. Very good agreement with the available experimental results is obtained. [S0556-2813(98)00807-3]

PACS number(s): 21.10.−k, 27.40.+z, 21.60.Cs, 23.40.−s

I. INTRODUCTION

A good deal of experimental and theoretical work has been devoted recently to the understanding of the properties of pf-shell nuclei, in particular, to the deformed region of $N\sim Z$ nuclei around ^{48}Cr. Shell model calculations in the full pf shell have been able to give a satisfactory description of a rich variety of observables for nuclei up to mass $A=52$ [1–3]. For heavier isotopes, shell model Monte Carlo techniques have been applied [4,5]. In some cases, very illustrative, detailed comparisons with ''state of the art'' mean-field calculations have been possible [6,7].

^{48}Cr plays a central role in this region because it has the maximum number of valence protons and neutrons in the $1f_{7/2}$ orbit, therefore exhibiting the maximum quadrupole coherence. It behaves as a rotor in the strong-coupling limit, and many predictions of the deformed shell model for the nuclei with one particle (hole) on top of it are recovered experimentally—and by the full pf-shell model calculations [2].

As an example, the yrast band of ^{47}V—a hole on ^{48}Cr—has $K=\frac{3}{2}^-$, and follows nicely the predictions of the hole-rotor strong coupling model. Recent experimental data [8] have extended our knowledge of the yrast band [9,10]; they are compared in Fig. 1 with the shell model calculations of Ref. [2]. While a $J=\frac{29}{2}^-$ state is located where it was predicted, $J=\frac{35}{2}^-$ is assigned to a state that we claim to be $J=\frac{33}{2}^-$. Similarly, the yrast band of ^{49}Cr (a particle on ^{48}Cr) that can be interpreted as having $K=\frac{5}{2}^-$, has also been extended up to $J=\frac{31}{2}^-$ [11], with the same quality of agreement. A natural next step is to look for bands of opposite parity, i.e., positive in the odd nuclei and negative in the even ones. These intruder bands have been measured recently, and their theoretical description will be the aim of

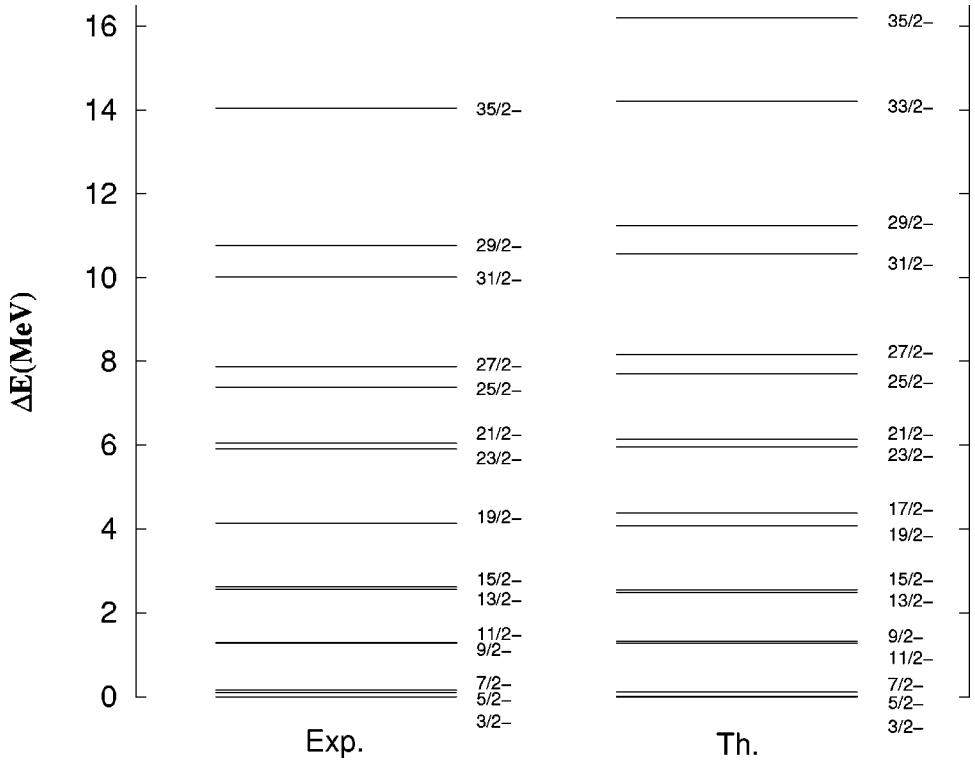

FIG. 1. Experimental and theoretical energy levels of the yrast band of ^{47}V.

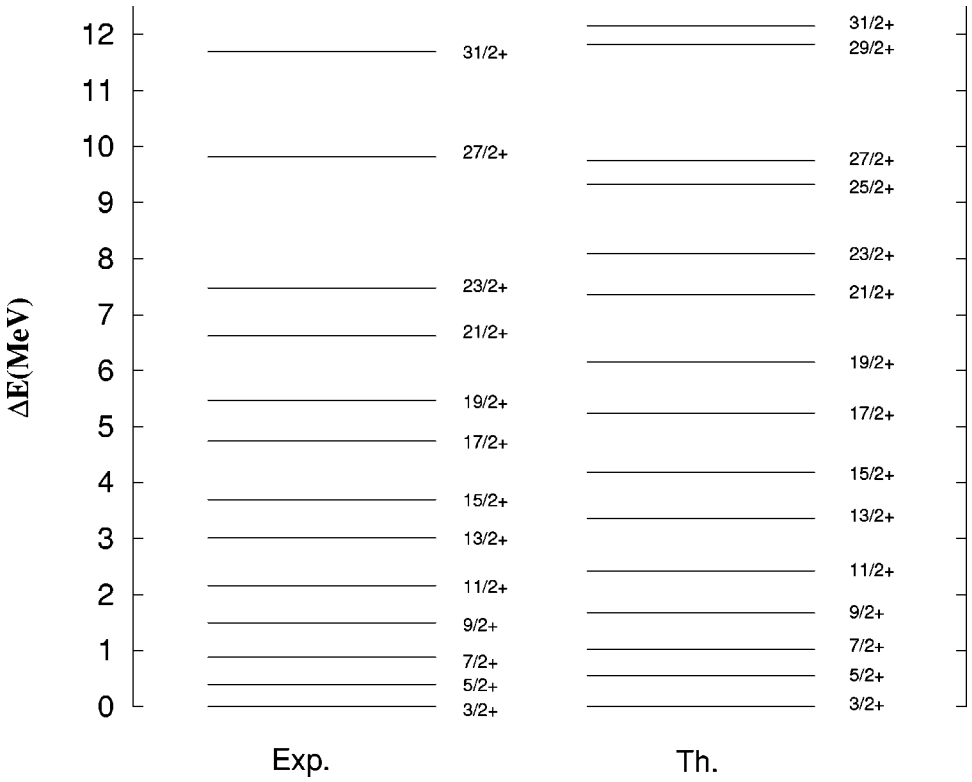

FIG. 2. Experimental and theoretical energy levels of the positive-parity intruder band of ^{47}V.

this paper. One such case, probably the most interesting one, is provided by ^{47}V, that has a positive-parity rotational band at very low excitation energy with band head $\frac{3}{2}^+$ [12]. The straightforward interpretation, that we will try to substantiate microscopically, is that the band results from the coupling of a proton hole in the $1d_{3/2}$ orbit to ^{48}Cr. A study along these lines has been recently performed for the positive-parity band of ^{45}Sc [13]. Its bandhead is almost degenerate with the

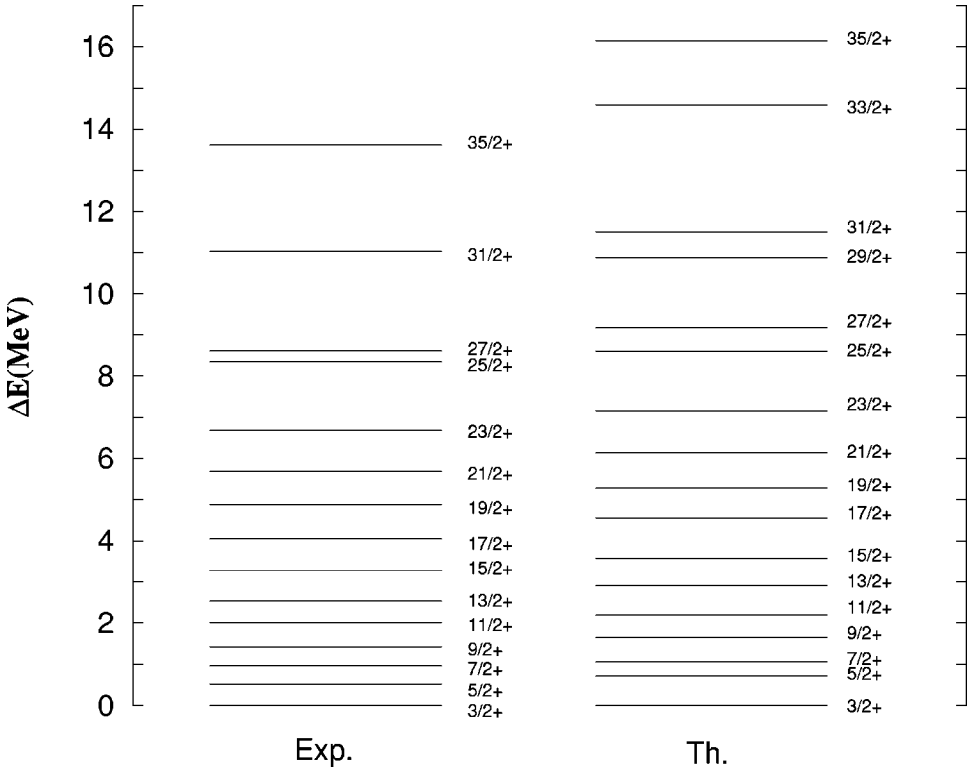

FIG. 3. Experimental and theoretical energy levels of the positive-parity intruder band of ^{45}Sc.

TABLE I. $E2$ and $M1$ reduced transition probabilities of the positive-parity states of ^{47}V. $B(E2)$ in e^2 fm^4 and $B(M1)$ in μ_N^2. Experimental values are from Ref. [12], except those bearing a star, which come from Ref. [16].

		$B(E2)$		$B(M1)$	
J^π(i)	J^π(f)	Expt.	Theor.	Expt.	Theor.
$\frac{5}{2}^+$	$\frac{3}{2}^+$		463.2	0.23(18)*	0.015
$\frac{7}{2}^+$	$\frac{3}{2}^+$	350(150)*	207.4		
$\frac{7}{2}^+$	$\frac{5}{2}^+$		323.7	0.09(3)*	0.023
$\frac{9}{2}^+$	$\frac{5}{2}^+$	240(30)*	284.4		
$\frac{9}{2}^+$	$\frac{7}{2}^+$		180.9	0.031(4)*	0.024
$\frac{11}{2}^+$	$\frac{7}{2}^+$	204(80)	350.0		
$\frac{11}{2}^+$	$\frac{9}{2}^+$		162.5	0.021(8)	0.029
$\frac{13}{2}^+$	$\frac{9}{2}^+$	<40	339.8		
$\frac{13}{2}^+$	$\frac{11}{2}^+$		79.1	<0.007	0.025
$\frac{15}{2}^+$	$\frac{11}{2}^+$	128(30)	368.0		
$\frac{15}{2}^+$	$\frac{13}{2}^+$		96.4	0.023(5)	0.031
$\frac{17}{2}^+$	$\frac{13}{2}^+$		324.7		
$\frac{17}{2}^+$	$\frac{15}{2}^+$		39.9		0.019
$\frac{19}{2}^+$	$\frac{15}{2}^+$	120(20)	329.4		
$\frac{19}{2}^+$	$\frac{17}{2}^+$		65.3	<0.04	0.019
$\frac{21}{2}^+$	$\frac{17}{2}^+$		223.7		
$\frac{21}{2}^+$	$\frac{19}{2}^+$		19.7		0.007
$\frac{23}{2}^+$	$\frac{19}{2}^+$	>200	205.5		
$\frac{23}{2}^+$	$\frac{21}{2}^+$		43.7		0.006
$\frac{25}{2}^+$	$\frac{21}{2}^+$		131.9		
$\frac{25}{2}^+$	$\frac{23}{2}^+$		20.8		0.0003
$\frac{27}{2}^+$	$\frac{23}{2}^+$	152(40)	147.8		
$\frac{27}{2}^+$	$\frac{25}{2}^+$		62.9		0.006
$\frac{29}{2}^+$	$\frac{25}{2}^+$		107.0		
$\frac{29}{2}^+$	$\frac{27}{2}^+$		13.9		0.002
$\frac{31}{2}^+$	$\frac{27}{2}^+$	73(15)	117.3		
$\frac{31}{2}^+$	$\frac{29}{2}^+$		45.9		0.001

ground state; we shall compute it for comparison as well. The ^{47}V case is a better one for two reasons: first, because ^{48}Cr is a much better rotor than ^{46}Ti and, second, because the effect of the ^{40}Ca core excitations is less important. As we shall show, the reason for these bands being so low in excitation energy is that the gain in correlation energy due to the excitation of one particle across $N=Z=20$ nearly compensates for the single-particle gap.

We shall use as valence space the pf shell without any truncation and a hole in the $1d_{3/2}$ orbit. We have also performed calculations in which the hole can be either in the $1d_{3/2}$ or $2s_{1/2}$ orbit, but the structure of the bands does not change appreciably. The effective interaction for the pf shell is KB3, the same one we used extensively in the $0\hbar\omega$ calculations [1]. For the cross-shell interaction we have taken the G matrix of Lee, Kahana and Scott [14] with the modifications of Ref. [15]. The largest m-scheme dimension we have treated is 13×10^6. We use harmonic-oscillator wave functions with $b=1.01A^{1/6}$ fm, bare electromagnetic factors in $M1$ transitions, and effective charges of $1.5e$ for protons and $0.5e$ for neutrons in the electric quadrupole transitions and moments.

We shall proceed as follows. Section II will be devoted to detailed spectroscopy by comparing calculations for both nuclei with the data in Refs. [16] and the recent results obtained by Cameron *et al.* [12] and Bednarczyk *et al.* [17]. In Sec. III, we will analyze the intrinsic structure of the positive-parity bands. Finally, conclusions will be given in Sec. IV.

II. LEVEL SCHEMES AND ELECTROMAGNETIC PROPERTIES

A. Energy levels

1. ^{47}V

The diagonalizations confirm our interpretation of the positive-parity band as overwhelmingly made up of the coupling of a proton hole to the even-even pf-shell configurations. The experimental and calculated levels for the positive-parity band for ^{47}V are plotted in Fig. 2. The yrast band roughly follows a $J(J+1)$ rotational behavior with a $K=\frac{3}{2}^+$ bandhead, in good agreement with the measured results. The position of the $J=\frac{3}{2}^+$ state relative to the ground state is in our calculation 1.5 MeV higher than the experimental one. Given that we have made no effort to adapt the cross shell interaction to this model space, this discrepancy is not unexpected. Our main goal is to study the structure of these bands, and to examine in detail why the excitation energy of the intruder bandhead is so low. With our effective interaction, the spherical mean-field energy difference between the negative and positive bands in ^{47}V is 7.9 MeV, whereas experimentally the excitation energy of the $J=\frac{3}{2}^+$ state is 260 keV. However, the correlation energy of the ground state, 12.1 MeV, is 6.1 MeV smaller than the correlation energy of the intruder bandhead leading to our predicted excitation energy of 1.8 MeV. The remaining discrepancy must be due to the overly large monopole gap between the sd and pf shells given by our effective interaction. The correlation energy of the intruder bandhead is very large (18.2 MeV), actually larger than the correlation energy we had in ^{48}Cr (15.6 MeV).

2. ^{45}Sc

The situation is even more striking in this nucleus, the intruders failing to become ground states by only 12 keV. In Fig. 3, we plot the experimental and calculated levels for the positive-parity band. The agreement is again quite good. The larger differences, that occur in the high-spin states, are of the order of 500 keV. The band follows the $J(J+1)$ rotational behavior with a $K=\frac{3}{2}^+$ bandhead. Notice that we locate a $J=\frac{33}{2}^+$ state at the place where an experimental $J=\frac{35}{2}^+$ level has been proposed. With respect to the position of the $J=\frac{3}{2}^+$ state relative to the ground state, our calculation places it 70 keV below the $J=\frac{7}{2}^-$, which represents a very good agreement. As for the discrepancy in the precedent case, we consider it as accidental. The monopole energy difference between the positive- and the negative-parity configurations (7.21 MeV) is in this case a bit overcompensated for by the gain in the correlation energy (7.28 MeV) owing to the presence of one extra particle in the pf shell. As in the vanadium case, the correlation energy of the head of the positive-parity band (12.04 MeV) is larger than the correlation energy of the ground state of ^{46}Ti (10.84 MeV).

TABLE II. Electromagnetic properties of the positive-parity band of ^{47}V. $B(E2)$ in e^2 fm^4, Q in e fm^2. Experimental values are from Ref. [12], except those bearing a star, which come from Ref. [16].

	$B(E2,J^\pi \to J^\pi-2)$		Q_0		
J^π	Expt.	Theor.	$Q_{\rm spec}$	from $Q_{\rm spec}$	from $B(E2)$
$\frac{3}{2}^+$			24.8	127.0	
$\frac{5}{2}^+$			−9.3	133.5	
$\frac{7}{2}^+$	350(150)*	207.4	−21.2	108.3	123.6
$\frac{9}{2}^+$	240(30)*	284.4	−34.8	130.4	118.1
$\frac{11}{2}^+$	204(80)	350.0	−33.4	107.2	120.2
$\frac{13}{2}^+$	<40	339.8	−43.1	125.8	113.0
$\frac{15}{2}^+$	128(30)	368.0	−34.5	94.7	114.2
$\frac{17}{2}^+$		324.7	−46.0	120.8	105.1
$\frac{19}{2}^+$	120(20)	329.4	−30.8	78.2	104.4
$\frac{21}{2}^+$		223.7	−31.3	77.4	85.1
$\frac{23}{2}^+$	>200	205.5	−9.5	23.0	80.9
$\frac{25}{2}^+$		131.9	−7.1	16.9	64.4
$\frac{27}{2}^+$	152(40)	147.8	4.7	−11.0	67.8
$\frac{29}{2}^+$		107.0	−14.3	33.3	57.4
$\frac{31}{2}^+$	73(15)	117.3	4.3	−9.9	59.9

TABLE III. Electromagnetic properties of the positive-parity band of ^{45}Sc. $B(E2)$ in e^2 fm^4, Q in e fm^2.

	$B(E2,J^\pi \to J^\pi-2)$	Q_0		
J^π	Theor.	$Q_{\rm spec}$	from $Q_{\rm spec}$	from $B(E2)$
$\frac{3}{2}^+$		5.2	93.6	
$\frac{5}{2}^+$		−1.8	91.9	
$\frac{7}{2}^+$	118.2	−3.2	58.9	91.9
$\frac{9}{2}^+$	156.0	−6.9	91.3	86.2
$\frac{11}{2}^+$	192.7	−5.6	63.4	88.0
$\frac{13}{2}^+$	180.1	−8.0	83.1	81.3
$\frac{15}{2}^+$	198.8	−6.0	58.5	82.7
$\frac{17}{2}^+$	164.1	−9.2	85.6	73.7
$\frac{19}{2}^+$	170.0	−6.7	60.3	73.9
$\frac{21}{2}^+$	119.4	−10.3	90.1	61.3
$\frac{23}{2}^+$	124.1	−6.0	52.0	61.9
$\frac{25}{2}^+$	29.5	−5.5	46.9	30.0
$\frac{27}{2}^+$	66.1	−4.4	36.4	44.7
$\frac{29}{2}^+$	25.8	−8.8	72.5	27.8
$\frac{31}{2}^+$	40.9	−4.1	33.5	34.8
$\frac{33}{2}^+$	1.1	−5.8	47.4	5.7
$\frac{35}{2}^+$	0.7	−6.5	52.5	4.6

B. Electromagnetic moments and transitions

In Table I, we list our predictions for the $E2$ and $M1$ transition probabilities compared with the available experimental values. For low and high spins our calculated $B(E2)$ values fit very well to the experimental ones. However, for $J=\frac{13}{2}^+$, $\frac{15}{2}^+$, and $\frac{19}{2}^+$, there are large discrepancies. Our values are consistent with what one should obtain in the rotational limit, that we expect to be valid up to $J=\frac{23}{2}^+$ in ^{47}V, because in ^{48}Cr—the core rotor—the reduction of the $B(E2)$'s begins only at $J=10^+$. The correct trend is recovered for the next spins, which makes the situation even more suspicious, and suggests that there is room for a new look to these experimental values. The $B(M1)$ compare reasonably well with the experimental data. There is almost no experimental information for the $E2$ and $M1$ transition probabilities in ^{45}Sc, hence we will only present some of our result in the context of Sec. III.

III. INTRINSIC STRUCTURE

A way to characterize a good rotor in the strong coupling limit [18] is to demand a $J(J+1)$ energy sequence *and* a constant intrinsic quadrupole moment Q_0 for all members of the band. In addition to being a constant, we expect Q_0 to be the same when extracted from the spectroscopic quadrupole moment through

$$Q_0=\frac{(J+1)(2J+3)}{3K^2-J(J+1)}Q_{\rm spec}(J) \quad \text{for } K\neq 1, \tag{1}$$

or from the $B(E2)$ transitions through the rotational model prescription (for $K\neq\frac{1}{2},1$)

$$B(E2,J\to J-2)=\frac{5}{16\pi}e^2|\langle JK20|J-2,K\rangle|^2Q_0^2. \tag{2}$$

Since ^{48}Cr is a reasonably good rotor at low spins, it is expected that the two mirror pairs obtained by adding and removing a particle from it (^{49}Cr-^{49}Mn and ^{47}V-^{47}Cr) would be well described by the strong-coupling limit particle plus rotor model and, in fact this is the case for the natural parity bands, as shown in Ref. [2]. Thus a similar situation is expected for the low-lying positive-parity bands in ^{47}V and ^{47}Cr.

The results of applying Eqs. (1) and (2) to the $K=\frac{3}{2}^+$ band obtained by allowing a single hole in the $1d_{3/2}$ subshell in the ^{47}V are gathered in Table II. The values of the intrinsic quadrupole moment are nearly constant for low spins, either the ones obtained from the spectroscopic quadrupole moments or the ones coming from the $B(E2)$'s. This last set is the most regular one, and the average value of Q_0, 110 e fm^2, is very close to (but slightly larger than) the average value of 100 e fm^2 we had in ^{48}Cr [1]. This corresponds to a deformation parameter $\beta\approx 0.35$. The reduction of Q_0 beyond $J=\frac{19}{2}^+$ in ^{47}V, is correlated with a similar reduction in ^{48}Cr beyond $J=8^+$.

We do not expect such a nice behavior in ^{45}Sc, mainly because the rotor status of ^{46}Ti is not as good as that of ^{48}Cr. In Table III, we show the quadrupole properties of the positive-parity band of ^{45}Sc and the intrinsic quadrupole moments extracted as explained above. It is seen that the differences between the Q_0 values extracted from the $B(E2)$'s and from the spectroscopic quadrupole moments are much larger than before. Again the Q_0's extracted from the $B(E2)$'s behave more regularly. However, a clear decreasing trend is evident even at low spins. Everything confirms that the rotational features are less evident. An average Q_0 of 80 e fm^2 comes out, a number larger than what would naively be expected from the coupling of a hole to the rotor provided by ^{46}Ti, the average Q_0 of their low-spin yrast states being just 60 e fm^2.

IV. CONCLUSIONS

We have shown that the low-lying (intruder) positive-parity bands of ^{47}V and ^{45}Sc can be explained in a shell model framework, using a valence space that comprises the full pf shell and allowing for a hole in the $1d_{3/2}$ orbit. We have interpreted these results in terms of the coupling of one hole to the intrinsic state of the corresponding even-even pf-shell nucleus with $A+1$ nucleons. In the ^{47}V case this picture is nicely fulfilled, certainly due to the fact that the $A+1$ nucleus is ^{48}Cr that is known to be a quite rigid rotor. The positive-parity band in ^{47}V exhibits an intrinsic state that is 10% more deformed than the ^{48}Cr one. In ^{45}Sc these features are already present though in a less developed way. We find in particular that: the intrinsic quadrupole moment has a stronger dependence on the J of the level; the Q_0 values extracted from the $B(E2)$'s are at variance with those obtained from the spectroscopic quadrupole moments, and the intrinsic quadrupole moment of the positive-parity band is 30% larger than the one of the even-even reference nucleus ^{46}Ti.

ACKNOWLEDGMENTS

This work was supported by DGES (Spain) Grant No. PB96-0053. The CCCFC (Universidad Autónoma de Madrid, Spain) provided part of the computer cycles employed in this work.

[1] E. Caurier, A. P. Zuker, A. Poves, and G. Martínez-Pinedo, Phys. Rev. C **50**, 225 (1994).
[2] G. Martínez-Pinedo, A. P. Zuker, A. Poves, and E. Caurier, Phys. Rev. C **55**, 187 (1997).
[3] C. A. Ur, D. Bucurescu, S. M. Lenzi, G. Martínez-Pinedo, D. R. Napoli, D. Bazzacco, F. Brandolini, D. M. Brink, J. A. Cameron, G. de Angelis, M. De Poli, A. Gadea, S. Lunardi, N. Mărginean, M. A. Nagarajan, P. Pavan, C. Rossi Alvarez, and C. E. Svensson, Phys. Rev. C (to be published).
[4] S. E. Koonin, D. J. Dean, and K. Langanke, Phys. Rep. **278**, 2 (1997).
[5] M. Honma, T. Mizusaki, and T. Otsuka, Phys. Rev. Lett. **77**, 3315 (1996).
[6] E. Caurier, J. L. Egido, G. Martínez-Pinedo, A. Poves, J. Retamosa, L. M. Robledo, and A. P. Zuker, Phys. Rev. Lett. **75**, 2466 (1995).
[7] G. Martínez-Pinedo, A. Poves, L. M. Robledo, E. Caurier, F. Nowacki, J. Retamosa, and A. Zuker, Phys. Rev. C **54**, R2150 (1996).
[8] J. A. Cameron, J. Jonkman, C. E. Svensson, M. Gupta, G. Hackman, D. Hyde, S. M. Mullins, J. L. Rodríguez, A. Galindo-Uribarri, H. R. Andrews, G. C. Ball, V. P. Janzen, D. C. Radford, D. Ward, T. E. Drake, M. Cromaz, J. H. DeGraaf, and G. Zwartz, Phys. Lett. B **387**, 266 (1996).
[9] J. A. Cameron, M. A. Bentley, A. M. Bruce, R. A. Cunningham, H. G. Price, J. Simpson, D. D. Warner, A. N. James, W. Gelletley, and P. Van Isacker, Phys. Lett. B **319**, 58 (1993).
[10] J. A. Cameron, M. A. Bentley, A. M. Bruce, R. A. Cunningham, W. Gelletley, H. G. Price, J. Simpson, D. D. Warner, and A. N. James, Phys. Rev. C **49**, 1347 (1994).
[11] C. D. O'Leary, M. A. Bentley, D. E. Appelbe, D. M. Cullen, S. Ertük, R. A. Bark, A. Maj, and T. Saitoh, Phys. Rev. Lett. **79**, 4349 (1997).
[12] J. A. Cameron, J. L. Rodríguez, J. Jonkman, G. Hackman, S. M. Mullins, J. C. Waddington, Lihong Yao, T. Drake, M. Cromaz, J. H. DeGraaf, G. Zwartz, H. R. Andrews, G. Ball, A. Galindo-Uribarri, V. P. Janzen, D. C. Radford and D. Ward, Phys. Rev. C (to be published).
[13] P. Bednarczyk *et al.*, Phys. Lett. B **393**, 285 (1997).
[14] S. Kahana, H. C. Lee, and C. K. Scott, Phys. Rev. **180**, 956 (1969).
[15] J. Retamosa, E. Caurier, F. Nowacki, and A. Poves, Phys. Rev. C **55**, 1266 (1997).
[16] Electronic version of Nucl. Data Sheets: telnet//bnlnd2.dne.bnl.gov (130.199.112.132), http://www.dne.bnl.gov/nndc.html .
[17] P. Bednarczyk, J. Styczeń, R. Broda, M. Lach, W. Mǫczyński, D. Bazzacco, F. Brandolini, G. de Angelis, S. Lunardi, L. Müller, N. H. Medina, D. R. Napoli, C. M. Petrache, C. Rossi Alvarez, F. Scarlassara, G. F. Segato, C. Signorini, and F. Soramel, Z. Phys. A (to be published).
[18] A. Bohr and B. R. Mottelson, *Nuclear Structure* (Benjamin, New York, 1975), Vol. II.